Egyptian Journal of Aquatic Biology & Fisheries
Zoology Department, Faculty of Science,
Ain Shams University, Cairo, Egypt.
ISSN 1110 – 6131
Vol. 29(4): 1041 – 1059 (2025)
www.ejabf.journals.ekb.eg

Validation of ERA5 Reanalysis Temperature Data Against *In-Situ* Observations: A Case Study of Alexandria Port, Egypt

Mohamed ElBessa[1, 2], Medhat NorElDin[1], Ahmed M. Khedr[1], Kareem Tonbol[1*]
[1]College of Maritime Transport and Technology, Arab Academy for Science, Technology and Maritime Transport, Abu-Qir, Alexandria, Egypt
[2] Oceanography Department, Faculty of Science, University of Alexandria, Alexandria, Egypt

***Corresponding Author: ktonbol@aast.edu**

ARTICLE INFO
Article History:
Received: May 20, 2025
Accepted: July 15, 2025
Online: July 19, 2025

Keywords:
Alexandria Port,
Air temperature,
ERA5 Reanalysis dataset,
Observed data,
port,
THI

ABSTRACT
Surface air temperature is a critical parameter for developing climate change mitigation and adaptation strategies, as it directly supports port operations, urban planning, and climate research aimed at understanding long-term climatic trends. This study evaluated the reliability and accuracy of the ERA5 reanalysis dataset for Alexandria Port by comparing it with observed data from the Alexandria coastal weather station over the period 2010 to 2020. The focus is on 2-meter surface air temperature (T2m), with data analyzed across hourly, monthly, and annual timescales. Results indicate that while ERA5 effectively captures general temperature patterns over Alexandria Harbor, it consistently underestimates surface temperatures. Statistical analyses, including correlation coefficients and error metrics, show a strong alignment with observed data but also reveal ERA5's limitations in representing localized and extreme temperature events. Notably, ERA5 displays a stronger positive warming trend than the observational record, highlighting discrepancies in trend estimation. These findings emphasize the importance of site-specific calibration to enhance ERA5's performance as a climate reference dataset for Alexandria Port. Improved reliability is particularly vital for stakeholders, policymakers, and local communities, who rely on accurate temperature data to develop targeted climate resilience strategies—including efforts to green port operations, protect critical infrastructure, preserve sensitive ecosystems, and strengthen community preparedness in the face of climate change.

INTRODUCTION

The Mediterranean Basin, spanning latitudes 30° to 49° N and longitudes 5° 50′ W to 36° E, stretches across parts of three continents—Africa, Asia, and Europe. This region is characterized by a distinctive climate, featuring mild to cool, wet winters and warm to hot, dry summers **(Khaled *et al.*, 2013; Caloiero *et al.*, 2018)**.

Alexandria, one of Egypt's most important coastal cities, is not only a major summer resort but also holds strategic economic significance. As the country's primary seaport, it handles nearly 90% of Egypt's import and export activities **(APA, 1978; APA, 1994)**. Harbors such as Alexandria's play a vital role in global commerce, supporting

economic growth, transportation infrastructure, and international trade development **(World Bank, 2010; Becker *et al.*, 2012)**.

The Western Harbor of Alexandria, located west of the city along Egypt's Mediterranean coastline, is a natural harbor encompassing approximately 31km². It connects to the open sea through a narrow strait, which shields the harbor from the predominant northwesterly winds, making it a safe anchorage zone. The harbor's average water depth is around 7 meters. Its origin is attributed to coastal subsidence prior to the Holocene, followed by a marine transgression. The continental shelf surrounding the harbor is primarily composed of calcareous marine deposits **(Butzer, 1960; Mostafa *et al.*, 2004)**.

Climate analysis is increasingly vital in the modern era. Systematic documentation of weather conditions enables the prediction of future climatic patterns on both local and global scales **(Manandhar *et al.*, 2019)**. This has direct implications for sectors such as agriculture, tourism, and renewable energy development **(Becken *et al.*, 2010)**. Given society's reliance on climate-informed decision-making, reliable weather measurements are essential. Among these, air temperature is one of the most widely observed and analyzed variables **(Wang *et al.*, 2021)**, measurable at the surface or via satellite.

The European Centre for Medium-Range Weather Forecasts (ECMWF) is a reputable intergovernmental organization supported by 35 countries, with a long-standing commitment to producing high-quality atmospheric reanalysis datasets. As outlined in Table (1), ECMWF's reanalysis efforts began in 1979 with the FGGE project (Global Atmospheric Research Program), followed by successive generations: ERA-15 (mid-1990s), ERA-40 (2001–2003), and ERA-Interim (2006–2019). The current generation, ERA5, represents a significant advancement in reanalysis, offering higher spatial resolution, improved data assimilation, and the inclusion of land surface, ocean wave, and ozone products **(Hersbach *et al.*, 2020)**. Despite its comprehensive nature, final ERA5 data products typically become available 2–3 months behind real-time.

Table 1. The ECMWF reanalysis data set generations

Reanalysis	**Period covered**	**Grid resolution**	**Assimilation scheme**	**IFS model cycle (year)**	**Reference**
ERA-15	1979- 1994	125 km	OI	13r4(1995)	Gibson *et al.* (1999)
ERA-40	1957- 2002	125 km	3D-Var	23r4(2001)	Uppala *et al.* (2005)
ERA-Interim	1979-2019	80 km	4D-Var	31r2(2006)	Dee *et al.* (2011)
ERA5	1950- Present	31 km	4D-Var	41r2(2016)	Hersbach, H. *et al.* (2020)

Note: OI=optimal interpolation; Var: variation; DA=Data Assimilation of 4D-Var).

The ERA5 reanalysis dataset has extended its historical coverage back to 1950, building on advancements in model performance and data assimilation. It replaces the now-discontinued ERA-Interim reanalysis, which ceased in August 2019, and is a core component of the Copernicus Climate Change Service (C3S) **(Thépaut *et al.*, 2018)**.

ERA5 provides improved representation of Essential Climate Variables (ECVs) and is hosted on the C3S Climate Data Store (CDS) **(Raoul *et al.*, 2017)**. Key enhancements include higher spatial and temporal resolution, the inclusion of 3-hourly uncertainty estimates, and additional output variables such as the 100m wind product. These are generated from a ten-member ensemble 4D-Var data assimilation system **(Bonavita *et al.*, 2016; Hersbach *et al.*, 2020)**.

ERA5 integrates observational data with physical modeling laws, utilizing a land surface data assimilation system weakly coupled to its 4D-Var system to estimate surface parameters such as air temperature. Compared to ERA-Interim, ERA5 demonstrates improved performance over land, especially in terms of surface air temperature accuracy **(Wang *et al.*, 2021)**.

1.1 Climate change context

Globally, surface temperatures have increased significantly. From 2011 to 2020, the average surface temperature rose (0.95 to 1.20°C) above the pre-industrial baseline (1850–1900), with land temperatures increasing by 1.34 to 1.83°C and ocean temperatures by 0.68 to 1.01°C. Between 2001 and 2020, the global temperature was on average 0.99°C higher than the pre-industrial level. The rate of warming since 1970 is the fastest for any 50-year period in the last 2,000 years **(IPCC, 2023)**.

Human activities are the dominant cause of this warming, with anthropogenic greenhouse gases (GHGs) contributing +1.0°C to +2.0°C, partially offset by aerosol-related cooling (0.0°C to -0.8°C). Natural influences such as solar and volcanic activity contributed only -0.1°C to +0.1°C, while internal climate variability added -0.2°C to +0.2°C **(IPCC, 2023)**.

Climate change, driven by fossil fuel use, deforestation, and industrial emissions, is a pressing global issue that affects ecosystems, infrastructure, human health, and economic stability **(IPCC, 2021)**. It exacerbates social inequalities, disproportionately impacting low-income and vulnerable communities **(UNFCCC, 2020)**. The complexity of climate challenges requires interdisciplinary collaboration: environmental scientists, economists, engineers, and social scientists all contribute to developing evidence-based strategies for climate adaptation and mitigation **(Ostrom, 2009; Tonbol, 2024)**.

1.2 Regional climate and green port sustainability

The Mediterranean Basin, spanning 30°–49°N and 5°50′W–36°E, is influenced by both mid-latitude cyclones and subtropical systems, particularly the Azores High and the Indian Summer Monsoon (ISM) **(Raicich *et al.*, 2003; Abdel-Basset & Hasanean, 2006; Tyrlis *et al.*, 2013)**. During summer, the ISM can drive hot, dry conditions across

the southeastern Mediterranean, while winter is shaped by interactions between the Siberian High, Azores High, and Mediterranean cyclones **(Nastos & Zerefos, 2009; De Vries *et al.*, 2013; Elbessa & Shaltout, 2024)**.

According to **Domroes and El-Tantawi** (2005), Alexandria's annual average surface temperature from 1941–2000 was 20.3°C, with a warming rate of 0.1°C per decade. Subsequent studies using ERA-Interim data reported an average of 20.0–20.5°C and warming rates of 0.3–0.4°C per decade **(Shaltout *et al.*, 2013)**. **Tonbol *et al.* (2018)** found significant monthly variation, with peak temperatures of 29°C in August and lows of 14°C in January, and a warming trend of 0.2–0.5°C per decade from 2007 to 2016. **Mahfouz *et al.* (2020)** and **El-Geziry *et al.* (2021)** observed hourly surface temperatures ranging from 7°C to 41°C and 5.2°C to 41.0°C, respectively, with annual means of 21.9°C, reinforcing the evidence of significant warming in the region.

In parallel, Alexandria Port, Egypt's primary seaport, handles nearly 90% of national trade and plays as a key role in the regional economy **(APA, 1978, 1994)**. The Western Harbor, with an area of ~31 km², benefits from protection via a narrow strait, forming a natural safe anchorage with an average depth of 7 meters **(Butzer, 1960; Mostafa *et al.*, 2004)**.

1.3 Green ports and sustainable development

The green port concept integrates environmental sustainability with economic functionality, aiming to reduce emissions, enhance energy efficiency, and protect ecosystems while maintaining high operational performance. Defined as a port that fulfills current needs without compromising future generations, green ports promote balanced development across environmental, social, and economic dimensions **(ESPO, 1995; Jiuh-Bing *et al.*, 2013)**.

A green port proactively implements measures to manage air, water, noise, and waste, often using clean energy, electric vehicles, onshore power supplies, and digital technologies to reduce its carbon footprint **(Acciaro *et al.*, 2014; Chen *et al.*, 2019)**.

As climate pressures intensify—especially in Mediterranean hot spots such as Alexandria—there is an urgent need to incorporate climate resilience into port planning and operation. Studies show the region is vulnerable to sea-level rise, urban heat, and weather extremes, requiring ports to adapt proactively **(Nicholls *et al.*, 2008; Mariotti, 2011; Mocerino *et al.*, 2018)**.

1.4 Importance of surface air temperature

Accurate surface air temperature data are essential for supporting climate adaptation, urban development, and operational planning in sectors such as transportation, renewable energy, and infrastructure resilience **(Becken *et al.*, 2010; Manandhar *et al.*, 2019)**. ERA5 provides hourly, high-resolution estimates that allow researchers to track localized trends, but biases in extreme events and urban heat underrepresentation require local calibration.

This study evaluated ERA5 surface air temperature accuracy over Alexandria Port, comparing it to observed weather station data (2010–2020) to assess its suitability for supporting green port strategies, climate resilience planning, and long-term environmental management.

MATERIALS AND METHODS

1. Material

1.1 Observed data

The Automated Weather Observation System was used to collect surface air temperature at Ras El-Tin Station, Alexandria Western Harbor. Details about this station are provided in Fig. (1) and Table (2). The Automated Weather Observation System (AWOS) was maintained according to WMO regulations, and all recorded data were calibrated to the standard height specified by the WMO. The dataset spans the years 2010 to 2020, with hourly measurements and no data gaps.

Table 2. Elevations and positions of the weather station at Ras El-Tin

Height above sea level (m)	Geographic position		International station number
	Latitude	Longitude	
21.95	31° 11` 50``	29° 51` 49``	62317

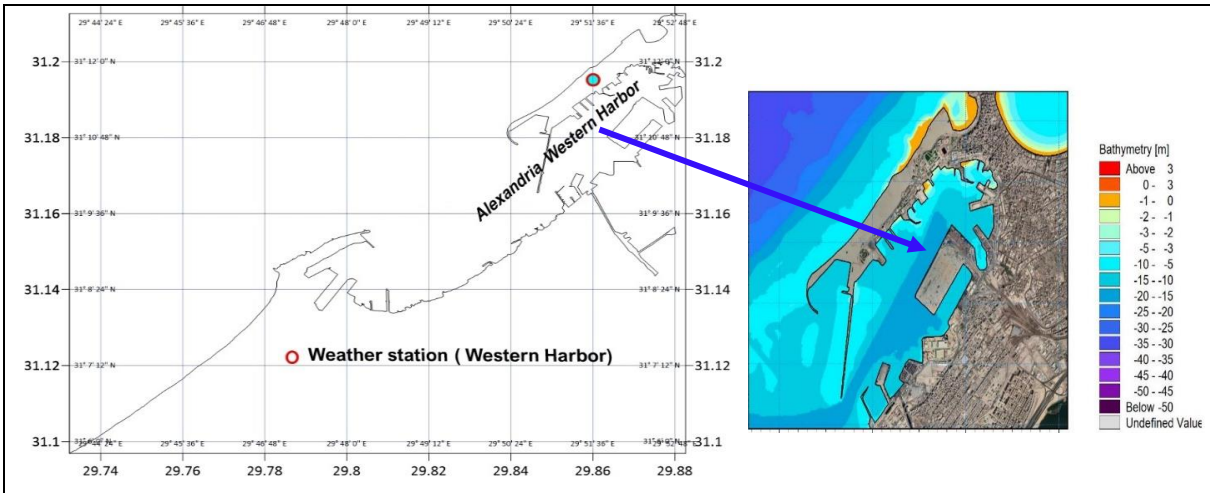

Fig. 1. The study area and position of the weather station at Ras El Tein, Alexandria

1.2 ERA5 database

The publicly accessible Copernicus Climate Change Service (C3S) provided hourly ERA5 single-level data for the period 2010–2020. This dataset includes key atmospheric variables such as 2-meter air temperature (T2m) and relative humidity (RH). ERA5, produced by the European Centre for Medium-Range Weather Forecasts (ECMWF) and distributed by C3S, represents a substantial improvement over earlier reanalysis versions, including ERA-Interim and ERA-40. These improvements include a

higher spatial resolution of 0.25° × 0.25° and an hourly temporal resolution, allowing for more detailed climate monitoring and analysis **(C3S, 2017; Hersbach *et al.*, 2020; Elbessa & Shaltout, 2024)**.

To tailor the gridded ERA5 data to specific points of interest, the dataset was downscaled using MATLAB (version 2024a). Spatial interpolation was performed using the griddedInterpolant function, with interpolation methods including bilinear, bicubic, and nearest-neighbor techniques. These methods were selected to ensure accurate estimation of atmospheric variable values at the station level, based on surrounding grid points.

Following validation with observational weather station data, ERA5 was confirmed as a reliable source for analyzing long-term trends in surface atmospheric variables. The validated data were subsequently used to assess ERA5's performance at the target location and to produce accurate, station-level products for further scientific analysis and climate-related applications.

2. Methods of analysis

2.1 Primary statistical analysis

The observed surface air temperature dataset was subjected to a series of descriptive statistical analyses to assess its temporal variability. Metrics including minimum, maximum, mean, and standard deviation were computed across hourly, daily, monthly, and annual time scales.

Anomaly detection

To identify temperature anomalies, comparisons were made between different temperature datasets and a selected baseline period, allowing for the detection of significant deviations from climatological norms.

2.2 Advanced statistical analysis

i. Relative humidity (RH)

To assess the effectiveness of ERA5 in estimating relative humidity (RH), hourly ERA5 values were directly compared with observed RH data at the station level. The analysis also included statistical hypothesis testing using two-sample t-tests to determine whether the means and variances of ERA5 and observed datasets were statistically identical—i.e., whether they could be considered to originate from the same population. A significance level of 95% was adopted for all tests.

Additionally, RH values were calculated from ERA5's 2-meter air temperature (T2m) using the formulation by **Alduchov and Eskridge (1996)**, as shown in Equation 1:

Equation 1:

$$RH = 100 \times (\exp[(17.625 \times Td)/(243.04 + Td)] / \exp[(17.625 \times T2m)/(243.04 + T2m)])$$

Where:

- *Td* = Dew Point Temperature (°C)
- *T2m* = Air Temperature at 2 meters (°C)
- RH = Relative Humidity (%)

This method is widely used for converting temperature data to relative humidity in climatological studies when dew point temperature is available or estimated.

THI (Temperature humidity index)

Relative humidity (RH) alone provides limited insight without the corresponding air temperature. Therefore, the Temperature–Humidity Index (THI), as proposed by **Liljegren *et al*. (2008)**, was employed to more effectively identify extreme heat stress events. The THI integrates both air temperature (T, °C) and relative humidity (RH, %) to evaluate human thermal comfort:

Equation (2):

$$THI = T - [(0.55 - 0.0055 \times RH) \times (T - 14.5)]$$

Where:

- T = Temperature at 2 meters (°C)
- RH = Relative Humidity (%)

THI Heat Stress Classification (Liljegren *et al*., 2008):

- **THI < 27°C**: Safe
- **27°C ≤ THI < 32°C**: Risk of heat fatigue with physical activity or extended exposure
- **32°C ≤ THI < 41°C**: Risk of heat exhaustion or sunstroke
- **41°C ≤ THI < 54°C**: Possibility of heat cramps and sunstroke
- **THI ≥ 54°C**: Danger of sunstroke, heat stroke, or delirium

2.4 Statistical evaluation metrics

To evaluate the performance of ERA5 reanalysis data against observed station data, several widely used error and correlation metrics were applied:

i. Bias

Bias measures the systematic deviation of reanalysis data from observed values. It quantifies whether ERA5 consistently over- or underestimates the variable.

Equation (3):

$$\textbf{Bias} = (1/n) \times \Sigma(Si - Oi)$$

Where:

- Si = ERA5 estimate
- Oi = Observed value
- n = Number of data points

ii. Root mean square error (RMSE)

RMSE evaluates the magnitude of prediction error between ERA5 and observed values. It is sensitive to large deviations:

Equation (4):

$$\textbf{RMSE} = \sqrt{[(1/n) \times \Sigma(Si - Oi)^2]}$$

iii. Mean absolute error (MAE)

MAE measures the average absolute error between model and observations, less sensitive to outliers than RMSE:

Equation (5):

$$\mathbf{MAE} = (1/n) \times \Sigma|Si - Oi|$$

iv. Scatter index (SI)

SI is a normalized error metric, defined as the RMSE divided by the mean of the observed values, and is typically expressed as a percentage. A lower SI indicates better model performance.

Equation (6):

$$SI = RMSE / \bar{O}$$

Where, $\bar{O}$ is the mean of the observed values.

v. Correlation coefficient (COR)

The Pearson correlation coefficient (r) quantifies the linear relationship between ERA5 and observed data. Values range from −1 to +1, where:

- **+1** = perfect positive correlation
- **0** = no correlation
- **−1** = perfect negative correlation

Equation (7):

$$\mathbf{COR} = \Sigma[(Oi - \bar{O})(Si - \bar{\mathbf{S}})] / \sqrt{[\Sigma(Oi - \bar{O})^2 \times \Sigma(Si - \bar{\mathbf{S}})^2]}$$

Where:

- *Oi, Si* = Observed and reanalysis values
- $\bar{\mathbf{O}}$, $\bar{\mathbf{S}}$ = Means of observations and reanalysis
- *n* = Number of paired values

These metrics collectively provide a comprehensive assessment of the ERA5 dataset's performance in representing surface air temperature and relative humidity over the study region. The incorporation of THI further strengthens the evaluation by detecting heat stress risks relevant for public health, infrastructure, and environmental planning.

RESULTS AND DISCUSSION

3. Observed data

3.1 Monthly time series

These values represent the monthly average surface air temperatures (T2m) at Ras El-Tin, calculated from hourly observed data spanning the period 2010–2020. As shown in Fig. (2), the coldest month on record was January 2019, with an average

temperature of 14.35°C, while the hottest month occurred in August 2015, with an average of 29.1°C.

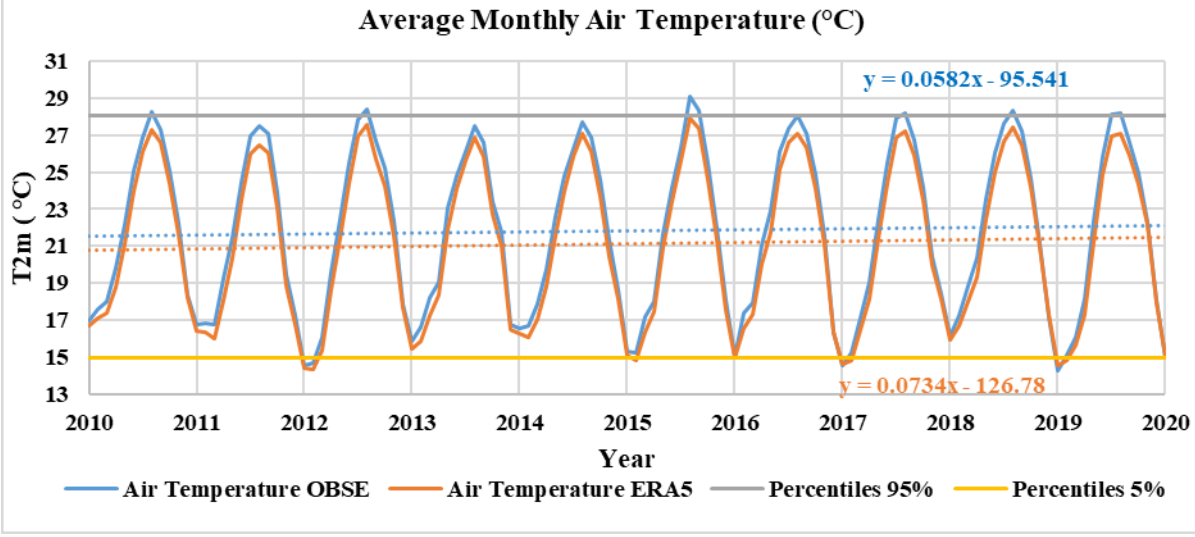

Fig. 2. The monthly average time series of surface air temperature understudy is derived from hourly observed data over Ras El Tin from 2010 to 2020

3.2 Hourly, monthly, and annual cycle

The hourly observed data reveal pronounced diurnal variations in surface air temperature (T2m) at Ras El-Tin. The highest average temperature, 23.69°C, was recorded at 13:00, while the lowest, 20.25°C, occurred at 04:00. These variations reflect the clear influence of the diurnal solar radiation cycle, as detailed in Table 3.

The monthly observed data illustrate a seasonal temperature cycle, with T2m peaking at a monthly average of 28.13°C in August and reaching a minimum of 15.53°C in January. This pattern reflects the typical transition between summer and winter, characteristic of the Mediterranean climate.

The annual temperature records for the period 2010–2020 show inter-annual variability in T2m. The highest annual average temperature, 22.40°C, was recorded in 2018, while the lowest, 21.50°C, occurred in 2011. These fluctuations suggest subtle but significant long-term climatic trends affecting the region over the past decade.

Table 3. Hourly, monthly, and annual characteristics of T2m derived from hourly observed data (2010–2020) over Ras El Tin station

	Parameters	**Surface air temperature (T2m, °C)**		
		Hourly	**Monthly**	**Annually**
Ras El Tin	**Max.**	**23.69 (13:00)**	**28.13 (AUG)**	**22.40 (2018)**
	Min.	**20.25 (04:00)**	**15.53 (JAN)**	**21.50 (2011)**

3.2.1 The annual cycle

The observed short-term monthly means presented in Fig. (3) reveal distinct seasonal patterns in surface air temperature (T2m), reflecting the climatic characteristics of the Ras El-Tin Station. The temperature trends align with typical Mediterranean climate behavior, marked by higher temperatures during the summer months and lower values in winter, consistent with seasonal shifts in atmospheric circulation and regional climatic drivers. The reanalysis datasets validated against these observations demonstrate a symmetric pattern, confirming their reliability in capturing seasonal temperature variability.

Similarly, the observed short-term hourly means, illustrated in Fig. (4), highlight the diurnal temperature cycle. Based on hourly observed data from 2010 to 2020, this daily cycle shows a clear pattern, with temperatures peaking in the early afternoon and reaching their minimum just before sunrise, further emphasizing the role of solar radiation and atmospheric dynamics in shaping local temperature fluctuations.

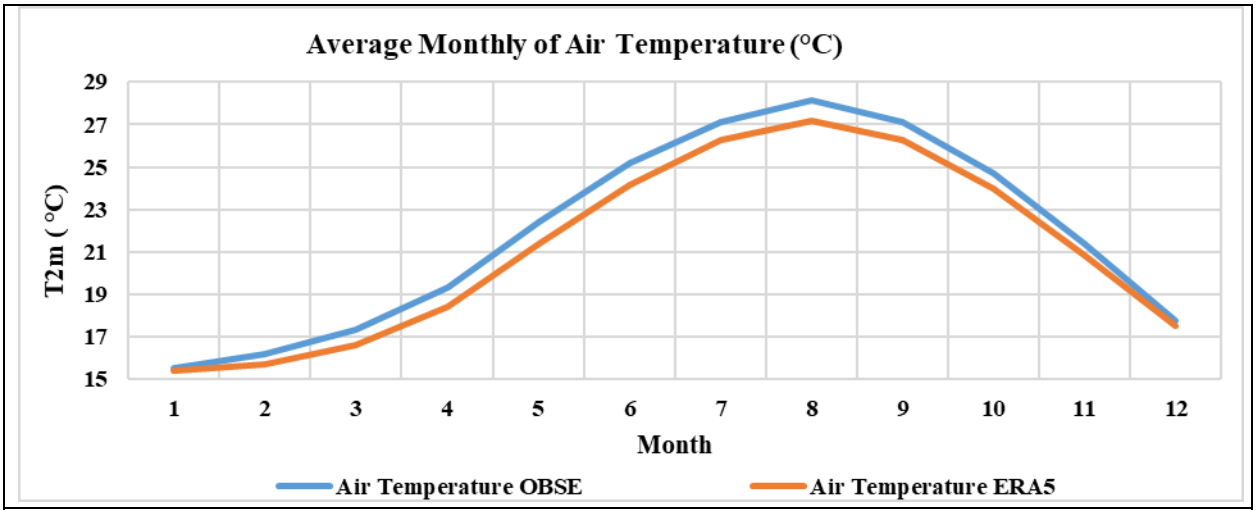

Fig. 3. The annual cycle (short-term monthly means) for T2m under study derived from hourly observed data from 2010 to 2020

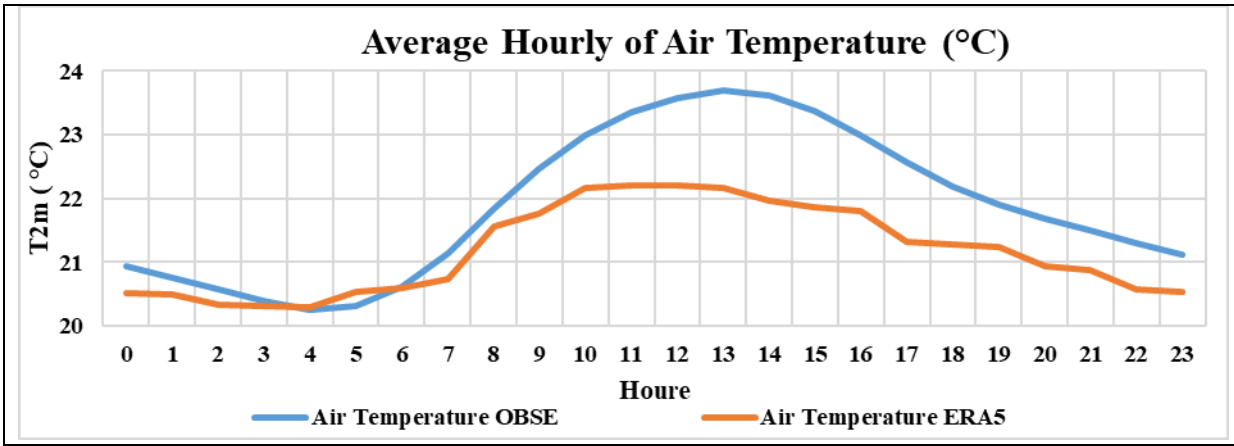

Fig. 4. The daily cycle (short-term hourly means) for T2m under study derived from hourly observed data from 2010 to 2020

3.2.2 The percentage of occurrences

During the hottest hours the percentage of occurrences (mean + 2 × standard deviation) is 0.72% (>30.9°C), at Ras El-Tein, as shown in Fig. (5a). In the same context, the percentage of occurrences for THI during extreme hourly events (mean + 2 × standard deviation) is 18.12% (>28.3°C) with standard deviation(mean) of ±4.09 (20.13) at Ras El-Tein, as shown in Fig. (5b). The values of THI and T2m were equivalent to the findings reported by **Elbessa and Shaltout (2024)**.

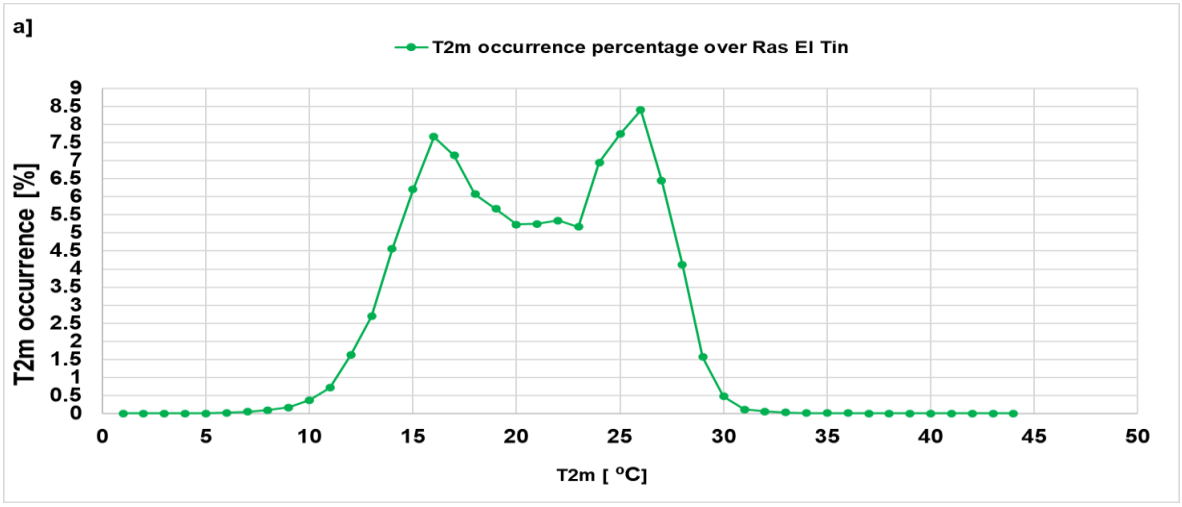

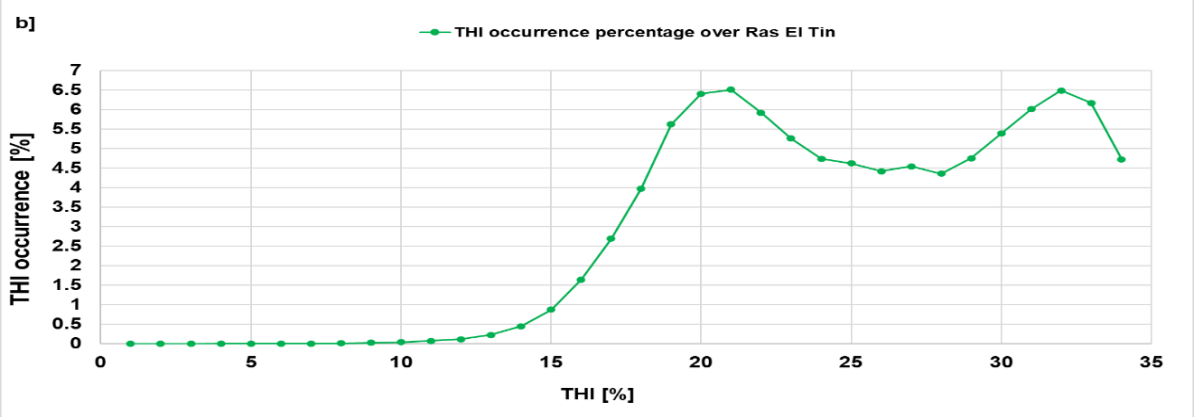

Fig. 5. The occurrence percentage of the T2m,and THI understudy based on hourly ERA5 dataset at Ras El Tein (2010-2020)

3.3 Evaluate the reliability of the ERA5 data set

To assess the suitability of using ERA5 for representing surface air temperature (T2m) over the Ras El-Tin Station, a comparative analysis was conducted between observed data and the ERA5 reanalysis dataset covering the period from 2010 to 2020, as summarized in Table (4).

The comparison reveals a strong correlation (R= 0.97) between the two datasets, indicating that ERA5 effectively captures the overall temperature variability across the study area. However, a consistent negative bias of -0.70°C suggests that ERA5 slightly underestimates actual surface temperatures. Furthermore, the observed data exhibit a broader range of extremes, with temperatures ranging from 7°C to 41°C, compared to the more constrained range of 8.2°C to 33.6°C in ERA5. This reflects the smoothing effect commonly associated with reanalysis datasets.

Both datasets show nearly identical skewness values (-0.1), indicating similar distributional symmetry. The annual mean temperature from ERA5 (21.2 ± 4.5°C) is slightly lower than the observed mean (21.9 ± 4.9°C), further supporting the conclusion of a systematic underestimation by ERA5.

Overall, while ERA5 reliably captures the seasonal and interannual temperature trends, caution is advised when using it for analyses involving temperature extremes or applications requiring precise absolute temperature values. Nevertheless, the strong agreement affirms that ERA5 data are well-suited for climatological assessments over the Ras El-Tin region.

Table 4. Comparison analysis between ERA5 and observed T2m over Ras El Tin (n = number of observations, R = correlation coefficient, St. dev.=standard deviation, and SK=Skewness)

Variables		**n**	**R [%]**	Bias	**Max.**	**Min.**	**Sk.**	**Annual mean ±St. dev.**
Surface air temperature (T2m, °C)	Obs.	122640	0.97	-0.70	41	7	-0.1	21.9/±4.9
	ERA5				33.6	8.2	-0.1	21.2/±4.5

3.3.1 Air temperature data

The comparison between observed and ERA5 air temperature data reveals key insights into the reliability of ERA5 data in replicating observed conditions. Table (5) summarizes the calculated error metrics: Bias, RMSE, MAE, and Scatter Index (SI).

Table 5. Error metrics for the comparison of ERA5 and observed air temperature data, including Bias, MAE (Mean Absolute Error), RMSE (Root Mean Square Error), and Scatter Index (SI)

Metric	**Value**
Bias	-0.70
Root Mean Square Error (RMSE)	1.28
Mean Absolute Error (MAE)	0.96
Scatter Index (SI)	0.06

The negative bias of −0.699 °C indicates that, on average, ERA5 surface air temperature data slightly underestimates observed values by approximately 0.7°C. This consistent underestimation reflects a systematic deviation, which may stem from factors such as spatial resolution limitations, modeling assumptions, or simplifications in the representation of atmospheric processes. Despite this, the magnitude of the bias remains relatively small, suggesting that ERA5 still offers a reliable approximation of actual temperature conditions at Ras El-Tin.

Moreover, the low values of RMSE (1.278°C) and MAE (0.957°C) indicate a strong overall agreement between the ERA5 and observed datasets. Specifically, an RMSE of 1.278°C implies that ERA5 predictions deviate only slightly from the observed values on average, while an MAE below 1°C demonstrates that the mean error across all data points is minimal. The Scatter Index (SI) of 0.058, which normalizes RMSE by the mean observed temperature, further confirms the high accuracy of ERA5, with the prediction error constituting only 5.8% of the mean observed value.

These metrics collectively underscore the robustness of ERA5 data, making it suitable for a wide range of applications, including climate monitoring, weather prediction, and environmental assessment.

Fig. (6) provides a visual comparison of observed versus ERA5 air temperature values. The scatter plot illustrates a strong clustering of points around the 1:1 line, with the red dashed line representing perfect agreement. While minor dispersion exists, the majority of data points align closely with the line, supporting the statistical findings and confirming that ERA5 serves as a dependable proxy for observed surface temperatures, albeit with slight underestimation.

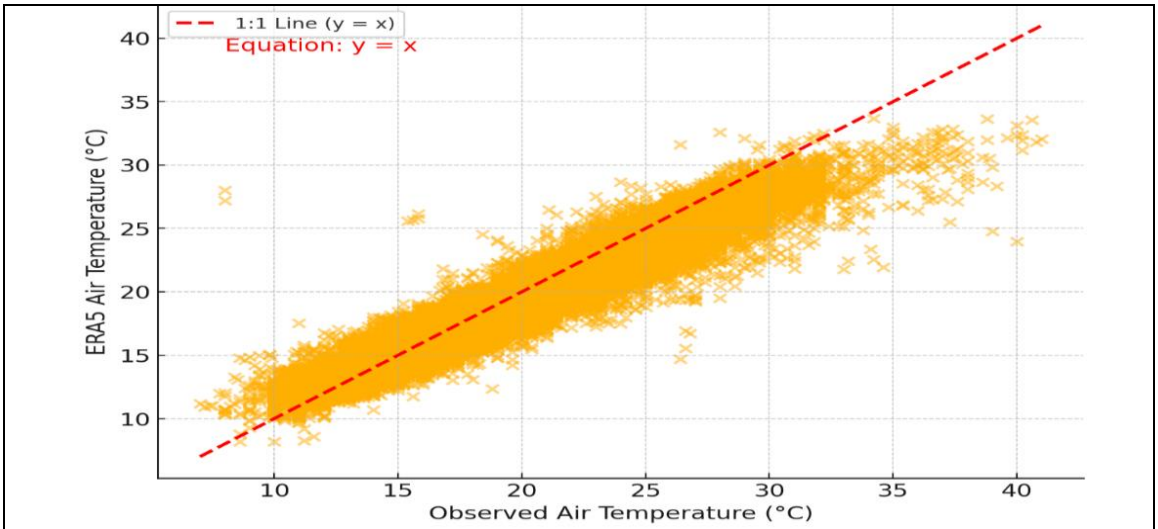

Fig. 6. Scatter plot comparing ERA5 air temperature data with observed air temperatures, with the red dashed line representing the 1:1 agreement line

3.3.2 Annual trend analysis

The annual trend analysis reveals differing trends between observed data and ERA5 data for four key parameters. The observed trend for temperature is 0.7, while the ERA5 trend is 0.9, both indicating an increase with ERA5 showing a slightly higher rise, as shown in Table (6).

These trends suggest that both datasets indicate a warming pattern over the study period, but ERA5 shows a slightly higher rate of warming. Moreover, both trends agree with the global warming report of the **IPCC (2023)**.

Table 6. Comparison between ERA5 and observed T2m over Ras El Tin for annual trend analysis

Variable	Obs. Trend (°C)	ERA5 Trend (°C)
Temperature	0.6984	0.8808

3.3.3 Historical days

The maximum T2m recorded in the study region was 41.00°C on June 21st, 2010, at 16:00 over Ras El-Tin. Conversely, the lowest T2m recorded 07.0°C on February 20th, 2015, at 02:00 over Ras El-Tin Station.

CONCLUSION

This study assessed the reliability of ERA5 reanalysis data by comparing it with observed surface air temperature records from the Ras El-Tin Station at Alexandria Port, Egypt, over the period 2010–2020. The findings demonstrate that while ERA5 performs well in capturing regional climate patterns and diurnal to seasonal temperature cycles, it consistently underestimates actual surface temperatures, particularly during extreme events. Although ERA5 effectively reproduces hourly, monthly, and annual temperature (T2m) trends, the smoothing effect on extremes limits its utility for operational decision-making and risk-sensitive applications where high precision is required.

Trend analysis revealed notable discrepancies in both the direction and magnitude of temperature changes between observed and ERA5 datasets. These differences underscore the necessity of localized calibration and validation to improve the accuracy of ERA5 in site-specific applications, such as port management and climate resilience planning.

Despite its limitations, ERA5 offers substantial value when integrated into sustainability frameworks, especially when accompanied by bias correction techniques. The dataset provides a robust foundation for understanding long-term temperature dynamics and for supporting climate-adaptive strategies in Alexandria Port. Future research should focus on enhancing ERA5 accuracy through refined bias correction models and exploring its utility under various climate scenarios.

In conclusion, ERA5 is a powerful tool for assessing regional climate variability and informing sustainable development, provided that local context and limitations are adequately addressed. Its application can aid stakeholders in mitigating climate-related risks, protecting infrastructure and workers, and promoting climate-resilient operations in the face of rising temperatures and environmental uncertainty.

REFERENCES

Acciaro, M.; Ghiara, H. and Cusano, M. I. (2014). Energy management in seaports: A new role for port authorities. *Energy Policy*, 71, 4-12. https://doi.org/10.1016/j.enpol.2014.04.013

Alduchov, O. and Eskridge, R. (1996). Improved Magnus Form Approximation of Saturation Vapor Pressure. *Journal of Applied Meteorology*, 35(4), 601-609. https://doi.org/10.2172/548871

Becker, A.; Inoue, S.; Fischer, M. and Schwegler, B. (2012). Climate change impacts on international seaports: knowledge, perceptions, and planning efforts among port administrators. *Climatic Change*, 110(1), 5-29.

Bonavita, M.; Holm, E.; Isaksen, L. and Fisher, M. (2016). The evolution of the ECMWF hybrid data assimilation system. *Quarterly Journal of the Royal Meteorological Society*, 142(694), 287-303.

Butzer, K. W. (1960). On the Pleistocene shorelines of Arab's Gulf, Egypt. *Egyptian Journal of Geology*, 68, 626-637.

Caloiero, T.; Veltri, S. and Frustaci, F. (2018). Drought Analysis in Europe and in the Mediterranean Basin Using the Standardized Precipitation Index. *Water*, 10, 1043. https://doi.org/10.3390/w10081043

Chen, S. L.; Jiuh-Bing, L. and Hsiao-Fang, C. (2019). Sustainable port development: A review of current practices and future directions. *Journal of Cleaner Production*, 207, 205-217.

Copernicus Climate Change Service (C3S). (2017). ERA5: Fifth generation of ECMWF atmospheric reanalysis of the global climate. Copernicus Climate Change Service Climate Data Store (CDS). https://cds.climate.copernicus.eu/cdsapp#!/home

De Vries, A. J.; Tyrlis, E.; Edry, D.; Krichak, S. O.; Steil, B. and Lelieveld, J. (2013). Extreme precipitation events in the Middle East: Dynamics of the Active Red Sea Trough. *Journal of Geophysical Research: Atmospheres*, 118(13), 7087-7108. https://doi.org/10.1002/jgrd.50569

Domroes, M. and El-Tantawi, A. (2005). Recent temporal and spatial temperature changes in Egypt. *International Journal of Climatology*, 25(1), 51-63. https://doi.org/10.1002/joc.1114

ElBessa, M. and Shaltout, M. (2024). Statistical Downscaling of Global Climate Projections along the Egyptian Mediterranean coast. *Oceanologia*, 66(4), 66401.

El-Geziry, T. M.; Elbessa, M. and Tonbol, K. M. (2021). Climatology of Sea-Land Breezes Along the Southern Coast of the Levantine Basin. *Pure and Applied Geophysics*, 178(5), 1927-1941. https://doi.org/10.1007/s00024-021-02726-x

European Sea Ports Organisation (ESPO). (1995). Sustainable port development: Balancing environmental, social, and economic dimensions. *European Sea Ports Organisation Policy Review*.

Hasanean, H. M. and Basset, H. A. (2006). Variability of summer temperature over Egypt. *International Journal of Climatology*, 26(12), 1619-1634.

Hersbach, H.; Bell, B.; Berrisford, P.; Hirahara, S.; Horányi, A.; Muñoz-Sabater, J.; Nicolas, J.; Peubey, C.; Radu, R.; Schepers, D. and Simmons, A. (2020). The ERA5 global reanalysis. *Quarterly Journal of the Royal Meteorological Society*, 146(730), 1999-2049. https://doi.org/10.5697/OBOE5006

Hongyuan, S.; Xuefeng, C.; Qingjie, L.; Delei, L.; Jiacheng, S.; Zaijin, Y. and Qingying, S. (2021). Evaluating the Accuracy of ERA5 Wave Reanalysis in the Water Around China. *Journal of Ocean University of China*, 20(1), 1-9.

IPCC. (2023). Summary for Policymakers. In: *Climate Change 2023: Synthesis Report*. Contribution of Working Groups I, II and III to the Sixth Assessment Report of the Intergovernmental Panel on Climate Change. IPCC, Geneva, Switzerland, pp. 1-34. https://doi.org/10.59327/IPCC/AR6-9789291691647.001

IPCC. (2021). *Climate Change 2021: The Physical Science Basis*. Contribution of Working Group I to the Sixth Assessment Report of the Intergovernmental Panel on Climate Change.

Jiuh-Bing, S.; Tung-Lai, H. and Su-Ru, L. (2013). The Key Factors of Green Port in Sustainable Development. *Pakistan Journal of Statistics*, 29(5), 755-768.

Khaled, A.; El Nemr, A. and El Sikaily, A. (2013). Heavy metals concentrations in biota of the Mediterranean Sea: a review, part I. *Blue Biotechnology Journal*, 2(1), 79.

Liljegren, J. C.; Carhart, R. A.; Lawday, P.; Tschopp, S. and Sharp, R. (2008). Modeling the wet bulb globe temperature using standard meteorological measurements. *Journal of Occupational and Environmental Hygiene*, 5(10), 645-655. https://doi.org/10.1080/15459620802310770

Mahfouz, B. M. B.; Osman, A. G. M.; Saber, S. A. and Kanhalaf-Allah, H. M. M. (2020). Assessment of weather and climate variability over the western harbor of Alexandria, Egypt. *Egyptian Journal of Aquatic Biology and Fisheries*, 24(5), 323-339. https://doi.org/10.21608/EJABF.2020.105861

Mahfouz, M.; El-Tantawi, A. and Shaltout, M. (2020). Temporal variability of atmospheric and marine parameters along the Mediterranean coast of Egypt. *Journal of Coastal Research*, 36(4), 812-820.

Manandhar, S.; Dev, S.; Lee, Y. H.; Meng, Y. S. and Winkler, S. (2019). A data-driven approach for accurate rainfall prediction. *IEEE Transactions on Geoscience and Remote Sensing*, 57(11), 9323-9331.

Mariotti, A. (2011). Decadal Climate Variability and Change in the Mediterranean Region. US National Oceanic and Atmospheric Administration, Climate Test Bed Joint Seminar Series NCEP, Camp Springs, Maryland.

Mostafa, A.; Barakat, A.; Qian, Y. and Wade, T. (2004). An overview of metal pollution in the Western Harbor of Alexandria, Egypt. *Soil and Sediment Contamination*, 13, 299-311.

Nastos, P. T. and Zerefos, C. S. (2009). Spatial and temporal variability of consecutive dry and wet days in Greece. *Atmospheric Research*, 94(4), 616-628. https://doi.org/10.1016/j.atmosres.2009.03.009

Nicholls, R. J.; Wong, P. P.; Burkett, V.; Woodroffe, C. D. and Hay, J. (2008). Climate change and coastal vulnerability assessment: scenarios for integrated assessment. *Sustainability Science*, 3, 89-102.

Ostrom, E. (2009). A general framework for analyzing sustainability of social-ecological systems. *Science*, 325(5939), 419-422.

Raicich, F.; Pinardi, N. and Navarra, A. (2003). Teleconnections between Indian monsoon and Sahel rainfall and the Mediterranean. *International Journal of Climatology*, 23(2), 173-186.

Saaroni, H.; Bitan, A.; Alpert, P. and Ziv, B. (1996). Continental polar outbreaks into the Levant and eastern Mediterranean. *International Journal of Climatology*, 16, 1175-1191. https://doi.org/10.1002/(SICI)1097-0088(199610)16:10<1175::AID-JOC79>3.0.CO;2

Saaroni, H.; Ziv, B.; Bitan, A. and Alpert, P. (1998). Easterly wind storms over Israel. *Theoretical and Applied Climatology*, 59(1-2), 61-77. https://doi.org/10.1007/s007040050013

Sallam, M. A. and Elsyed, M. A. (2015). An evaluation of climate parameters over Alexandria: Observational and reanalysis perspectives. *Climate Dynamics*, 44(3), 809-824.

Shaltout, M.; El Gindy, A. and Omstedt, A. (2013). Recent climate trends and future scenarios in the Egyptian Mediterranean coast based on six global climate models. *Geofizika*, 30(1), 19-41.

Shaltout, M.; Tonbol, K. and Mahfouz, M. (2013). Climate variability in the Mediterranean region: Observations and reanalysis perspectives. *Climate Dynamics*, 41(5-6), 1161-1173.

Thépaut, J. N.; Dee, D.; Engelen, R. and Pinty, B. (2018). The Copernicus Programme and its climate change service. In *IGARSS 2018 IEEE International Geoscience and Remote Sensing Symposium* (pp. 1591-1593). IEEE.

Tonbol, K. (2024). Climate change: interdisciplinary solutions for a global challenge. *Multidisciplinary Adaptive Climate Insights*, 1(1), 1-10.

Tonbol, K.; El-Geziry, T. and Elbessa, M. (2018). Evaluation of changes and trends in air temperature within the Southern Levantine basin. *Weather*, 73(2), 60-66.

Tyrlis, E.; Lelieveld, J. and Steil, B. (2013). The summer circulation over the eastern Mediterranean and the Middle East: influence of the South Asian monsoon. *Climate Dynamics*, 40, 1103-1123.

UNFCCC. (2020). *Climate Change: Impacts, Vulnerabilities, and Adaptation in Developing Countries*. United Nations Framework Convention on Climate Change.

Wang, C.; Graham, R.; Wang, K.; Gerland, S. and Granskog, M. (2019). Comparison of ERA5 and ERA-Interim near-surface air temperature, snowfall, and precipitation over Arctic Sea ice: effects on sea ice thermodynamics and evolution. *The Cryosphere*, 13(6), 1661-1679.

Zerefos, C.; Repapis, C.; Giannakopoulos, C.; Kapsomenakis, J.; Papanikolaou, D.; Papanikolaou, M.; Poulos, S.; Vrekoussis, M.; Philandras, C.; Tselioudis, G.; Gerasopoulos, E.; Douvis, K.; Diakakis, M.; Nastos, P.; Hadjinicolaou, P.;

Xoplaki, E.; Luterbacher, J.; Zanis, P.; Tzedakis, C. and Repapis, K. (2011). The climate of the Eastern Mediterranean and Greece: past, present, and future. In: *The Environmental, Economic and Social Impacts of Climate Change in Greece*. Bank of Greece, Athens, pp. 1-126.